2022 NIST Center for Neutron Research School
on Small Angle Neutron Scattering and Neutron Reflectometry

NG7 SANS
Self-assembly in binary lipid mixtures

Abstract

We will use small angle neutron scattering (SANS) to study the structure and composition of assemblies formed by binary mixtures of long- and short- tail lipids. The measurements will illustrate the advantage of using contrast matching in neutron scattering as well as introduce data treatment and analysis. The effects of mixing different amphiphilic molecules on the structure of the assemblies as well as the design of the SANS experiment are introduced here. References are given for more in-depth information.

1. Introduction

Lipid assemblies are found throughout cells in nature and in numerous products we encounter in our everyday lives from food to personal care products and even drug products and vaccines. Lipids are a type of amphiphilic molecule, with a hydrophilic – or water-loving – headgroup and hydrophobic – or water-hating – tails. In water, lipids form a wide variety of nanoscale structures where the hydrophilic headgroups are exposed to the aqueous environment and shield the inner hydrophobic core.

This self-assembly is the basis of biomembranes that compartmentalize cells, where the hydrophobic lipid tails form a low dielectric oil that hosts transmembrane proteins and prevents free passage of polar and charged species into and out of the cell (**Fig. 1**). The formation of well-defined hydrophobic pockets in an otherwise aqueous environment is also why lipid assemblies are used as containers for membrane proteins for protein structure determination measurements and for hydrophobic guest molecules in personal care products and drug delivery vehicles.
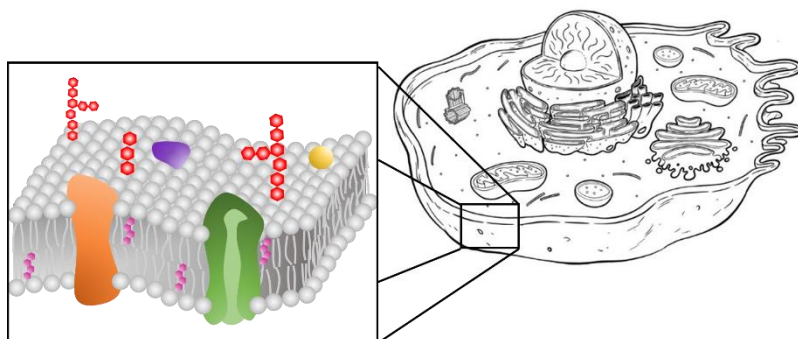

Figure 1. Cartoon illustration of a cell encapsulated and compartmentalized by membranes formed by self-assembled lipids

One type of self-assembled lipid structure that is widely used in biochemical and biophysical studies are "**bi**layed m**icelles**" or **bicelles** for short. Bicelles are easily aligned in a magnetic field, making them a useful tool for the nuclear magnetic resonance (NMR) based protein structure determination and studies of membrane associated peptides and proteins.(1, 2) More recently it was also demonstrated that the proton pump transmembrane protein bacteriorhodopsin could be crystallized from suspension in these lipid mixtures(3, 4) and their use has even expanded to topical drug delivery.(5)

One of the most widely used bicellar systems is a mixture of long tail 14-C dimyristoyl-phosphatidylcholine (DMPC) and shorter 6-C tail dihexanolyl-phosphatidylcholine (DHPC) lipids (see **Fig. 2** for corresponding structures).(6) DMPC and DHPC have identical phosphocholine (PC) headgroups and double chain carbon tails of 14 and 6 carbons per tail, respectively. However, variations in lipid ratio, lipid concentration, and even temperature can have profound effects on the resulting structures.

DMPC   **DHPC**

Figure 2. Molecular structures of DMPC and DHPC

1.1. Molecular shapes and the assemblies they form

In this experiment we will study the study the structures formed by mixing a long-tail lipid, DMPC, and a short-tail lipid, DHPC. At certain conditions, these lipid mixtures are reported to form bicelles that are widely used as model membrane systems.

So what determines the structure of self-assembled systems? While there are different ways to think about this, including thermodynamic frameworks,(7, 8) the simplest - yet very powerful - approach is a *geometric one*.(9, 10) Fundamentally, the structures formed are determined by the mean packing shape of the molecule (**Fig. 3**).(9, 10) Depending on the relative sizes of the hydrophobic and hydrophilic portions of the lipids, they can form a wide variety of structures from spherical micelles to rodlike micelles, to bilayers and vesicles, and even more complex inverted micellar structures that are important for example in some of the more complex membrane structures found in cells. These differences in molecular shape can be quantified by the critical
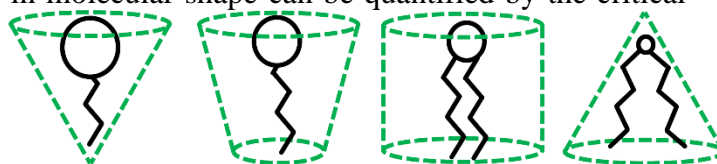
Figure 3. Amphiphilic molecules come in all sorts of shapes and sizes that self-assembly into a wide variety of structures depending on their critical packing parameter (CPP)

critical packing parameter	< 1/3	1/3 < CPP < 1/2	1/2 < CPP ≈ 1	CPP > 1
structures formed				

packing parameter (CPP, sometimes known as the surfactant packing parameter or SPP). CPP = $v/a_0 l_c$ where v is the molecular volume, a_0 is the area per molecule, and l_c is the length of the hydrocarbon tails.(10) A CPP $\leq$ ⅓ leads to spheres, ⅓ < CPP < ½ to rodlike elongations, CPP ~ 1 to bilayers (including vesicles) and CPP > 1 to "inverted" structures. Thus the CPP tells us something about the intrinsic preferred curvature in the structures formed.

Comparing the molecular shapes of DMPC and DHPC reveals that they have a very different CPP and therefore prefer to form different structures (**Fig. 4**). With a long tail relative to the size of the PC headgroup, DMPC has a large CPP close to 1 and forms flexible bilayers like those found in the cell membrane.(11) Meanwhile, because of the short tails, DHPC self-assembles into small spheroidal micelles in solution.(12)

The role of thermodynamics. Keep in mind that while the CPP tells us about the intrinsic curvature and what shape structures to expect, the driving force to actually create these aggregates, rather than the molecules being dissolved in solution or aggregating uncontrollably and precipitating out of

Figure 4. Mean shapes of lipids with different tail lengths and the structures they form

solution, is the details of the system energetics: thermodynamics. The shape of the self-assembled structure is thus the minimum energy state, but without covalent bonds the individual amphiphile molecules are free to move about within kT of the minimum energy structure. The consequence is that the self-assembled systems are not "frozen" shapes but actually undergo constant deformations from the nominal, idealized shape. Furthermore, the self-assembled structures can grow and shrink by insertion and ejection of individual amphiphilic molecules, leading to a polydispersity in the size of the structures formed. It is thus important to remember when measuring such systems that there is actually a distribution of sizes and shapes, not a single frozen one. This is where a bulk technique like scattering (and luckily this is a scattering school) that directly measures the statistically relevant average of that ensemble becomes a critically important tool.

What happens when we mix DMPC and DHPC? As one might guess, typically when mixing amphiphiles with very different CPP, the structures formed are based on an average CPP (strictly speaking the CPP of a stoichiometric ratio of the different molecules). Once again, the dynamic nature of the assembly has consequences. Indeed, it can induce transient local enrichment in one or the other amphiphile, leading to enhanced local curvatures which gives rise to much more dynamic self-assembled structures, e.g. sponge phases.(13, 14) However, there is a large body of literature that suggests at least certain DMPC/DHPC mixtures under certain conditions form relatively monodisperse discotic micelles, termed bicelle in the lipid literature (**Fig 5**).(15, 16) The
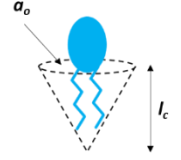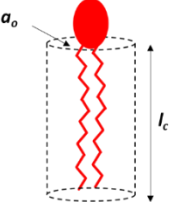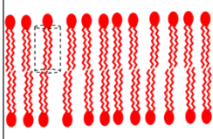
explanation is that the high CPP DMPC molecules segregate into a planar bilayer portion of the bicelle while the high intrinsic curvature DHCP molecules (small CPP) segregate into the curved rim, thereby decreasing the edge energy by protecting the hydrophobic tails from the surrounding solvent. Assuming that the minimum energy for these mixtures is the bicelle despite the high entropic cost of segregation, the question remains as to what extent to the lipids actually separate? Is the rim mainly purely of DHPC? Does some DHPC get trapped in the bilayer region? There is believed to be some degree of lipid mixing and a "mixed bicelle" model has therefore been proposed.(17-19) However, the degree of mixing has proven difficult to quantify. *The precise quantification of mixing, or lack thereof, the key component to understanding the underlying physics and chemistry, and, in turn, the structures of bicelles, would allow for better control and very specific tunability.*
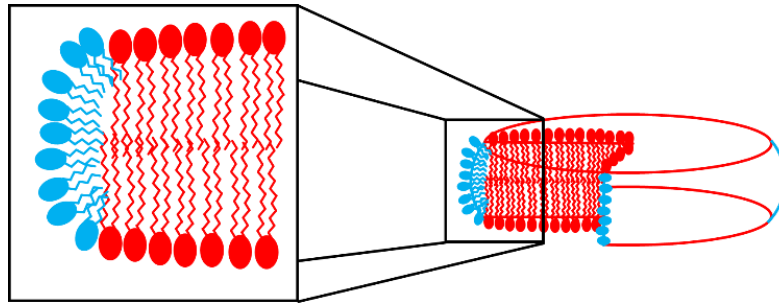

Figure 5. Cartoon illustration of a bicelle formed by mixtures of lipids with long- and short tails.

1.2. SANS from colloidal solutions: measuring the structure and composition of particles

The previous section suggested that mixing these two lipids, with different critical packing parameters and molecular shapes, leads to the assembly of new structures, but how do we confirm that the cartoons are accurate representations of the structures? And if they are, to what extent do the lipids segregate? How do we know which lipids go where? And finally, to the extent the lipids are segregating in some fashion, what is the physics/chemistry that drives that? As you might have guessed, being at a neutron scattering summer school – we can measure these structures and the degree of lipid mixing with small angle neutron scattering (SANS). But how does scattering from a solution tell us about the structure and composition of bicelles?

The coherent scattering intensity, *I(q),* from a monodisperse colloidal solution can be expressed as

$$I(q) = \phi V \Delta \rho^2 P(q) S(q) \qquad [1]$$

Where ϕ is the particle volume fraction, *V* is the particle volume, *Δρ* is the difference in scattering length density between the particles and the solvent, also called the scattering contrast, *P(q)* is the form factor and *S(q)* is the structure factor. In all of these expression *q* is the scattering vector which is given by $q = 4\pi/\lambda \sin\theta$ where 2θ is the scattering angle. The goal of every elastic scattering experiment is to measure the structures and interactions in the samples. To do this, we

need to determine the contrast, form factor and structure factor for our sample. We will discuss each of these terms in the next 3 sections.

1.2.1. Scattering contrast: $\Delta\rho^2$

To have enough scattered intensity to characterize the sample, there must be scattering contrast ($\Delta\rho$) between the sample and the surrounding solvent. In other words, the sample must 'look' different from the solvent as far as the neutrons are concerned. This is very similar - and in fact is related to - the index of refraction in light, where one needs a difference in index of refraction to "see" an object as separate from the matrix.

Neutrons interact with the nucleus of the of an atom and the probability that the neutron will interact with a given atomic nucleus is characterized by the so-called scattering length, b_i. The scattering length varies by element and by isotopes within a given element, which is a unique advantage of neutron scattering. Scattering by X-rays will increase with the atomic number while the neutron scattering length varies seemingly randomly across the periodic table. The b_i values for the elements and their isotopes are tabulated and can be found on the NCNR website: https://www.ncnr.nist.gov/resources/n-lengths/

That said, we are interested in length scales that are much larger than atomic distances in small angle scattering, so it is useful to define the scattering length density (SLD), ρ of a material,

$$\rho = \sum_i^N \frac{b_i}{V} \qquad [2]$$

In which V is the volume containing the N atoms. Calculating the SLD averages the scattering length over the volume of the material, and we are most interested in the differences in materials properties ρ_1 and ρ_2 where 1 and 2 are for example our particles and solvent, respectively. We refer to the difference in SLDs as the scattering contrast, $\Delta\rho = \rho_1 - \rho_2$. The larger the $\Delta\rho$, the larger the intensity. The SLD's can be calculated by hand from the tabulated values of b_i or by using the NCNR online calculator: https://www.ncnr.nist.gov/resources/activation/

Shown in Table 1 are calculated values for the SLD of DMPC, deuterated DMPC (d-DMPC), DHPC, D_2O and H_2O, the materials we will be using in our experiment. Notice that the ρ values for H_2O and D_2O differ by an order of magnitude and by sign. The difference is because hydrogen and deuterium have very different scattering lengths despite being isotopes (remember b_i varies with element *and* isotope). This means that we can vary the H and D content in our samples to change the scattering contrast for different components. In fact, it is often possible to find conditions where we match the SLD of the solvent to one of the components of the sample, a technique referred to as contrast matching. Contrast matching is a unique advantage of neutron scattering compared to other scattering techniques and makes SANS a very powerful tool for studying multicomponent systems – such as the ones we are interested in studying in this experiment.

Material	Chemical formula	Mass density @ 10 °C (g/cm³)	Scattering length density (cm⁻²)
DMPC	$C_{36}H_{72}NO_8P$	1.08	0.30×10^{10}
d-DHPC	$C_{36}H_5D_{67}NO_8P$	1.19	7.00×10^{10}
DHPC	$C_{20}H_{40}NO_8P$	1.16	0.67×10^{10}
Heavy water	D_2O	1.11	6.34×10^{10}
Light water	H_2O	1.00	-0.56×10^{10}

Table 1. Calculated scattering length densities for the materials we will be using in our experiment. Note that the values for silica and PEG are based on densities from literature and may not be precise. In particular, the silica density can vary with particle preparation method.

To study the structures formed by mixtures of DMPC and DHPC, we need to make sure there is enough contrast with the surrounding solvent to be able to see them. Contrast between the deuterated lipid and light water $\Delta\rho^2 = \left(\rho_{d-DMPC} - \rho_{H_2O}\right)^2 \approx (8.11 - (-0.561))^2 \approx 75$ is almost two times greater than the contrast between a protiated lipid and heavy water $\Delta\rho^2 = \left(\rho_{DMPC} - \rho_{D_2O}\right)^2 \approx (0.29 - 6.34)^2 \approx 36$. However, maximizing contrast is not the only thing we need to consider. We also need to consider the incoherent scattering (or background). Incoherent scattering contributes an isotropic (*i.e.* flat) background that can make it difficult to resolve the signal of interest at high *q* or short length scales. In the case of water, the incoherent scattering from H_2O is about 30 times greater than that from D_2O! Because hydrogen contributes an extremely large incoherent background compared to deuterium, the general rule of thumb in neutron scattering is to always make the majority component (usually the solvent in colloidal systems) deuterated and the minority component hydrogenated - at least in the absence of other considerations. Finally, it is important to note that deuterated versions of molecules are almost always more expensive than the protiated version (by a factor of ~ 1000 in the case of lipids used here) so cost can sometimes also be a consideration. Given that h-lipids are significantly cheaper than d-lipids, and that the majority component is water, we will do the experiments to determine the overall structure of the sample with h-lipids in D_2O.

Now, how do we figure out which lipids go where in the bicelle? Comparing the scattering length densities of DMPC and DHPC suggest they look very similar as far as the neutrons are concerned. Fortunately, we can take advantage of the difference in scattering length densities between h- and d-lipids and be clever about designing the contrast in our experiment. As shown in **Fig. 6**, we should be able to distinguish between d-DMPC from DHPC and figure out if the lipids evenly mix or segregate in the bicelles.
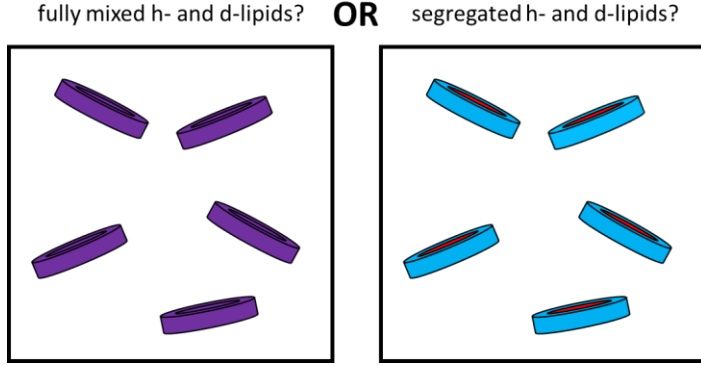
fully mixed h- and d-lipids? **OR** segregated h- and d-lipids?

Figure 6. Cartoon illustration of potential bicelles structures where d-DMPC and h-DHPC are mixed or segregated to the rim and bilayer regions as expected as seen in contrast-variation experiments with SANS.

1.2.2. Form Factor: *P(q)*

The form factor is scattering from interference from different parts of the same object and therefore provides information on the structure of the scattering object. *P(q)* is related to the Fourier transform of the real space density distribution,

$$P(q) = \left| \frac{1}{V_p} \int_{V_p} e^{-iq\vec{r}} \, d\vec{r} \right|^2 \qquad [3]$$

In the limit $q \to 0$, the above expression can be simplified for randomly oriented monodisperse particles, independent of their shape, by using a Taylor series expansion around 0. When truncated to the first term, this Taylor series expansion yields

$$I(q \to 0) \propto \exp\left(\frac{-q^2 R_g^2}{3} \right) \qquad [4]$$

Where R_g is the radius of gyration of the particle.

$$R_g^2 = \frac{\sum_i \rho_i (r_i - r_0)^2}{\sum_i \rho_i}$$

Where the mass term in the classical mechanics definition has been replaced with the SLD and r_0 is the SLD center of mass. The radius of gyration can thus be fairly easily calculated for various shapes. For example, for a homogenous sphere with radius R, $R_g^2 = 3R^2/5$, for a cylinder with

length L and radius R, $R_g^2 = L^2/12 + R^2/2$, and for an ellipsoid with axes lengths a, b, and c, $R_g^2 = (a^2 + b^2 + c^2)/5$.

The above equation is an example of Guinier's Law and, as we are truncating at the first term in the expansion, is valid only for very small qR_g. A typical rule of thumb is that $qR_g < 1$. More importantly, Eq. 4 can be used to estimate the particle size independent of any assumption of the shape and without needing a detailed form factor by simply plotting $\ln(I)$ versus q^2 at low q.

To extract more detailed information on the structure of the assemblies, an appropriate form factor model is needed. Fortunately, models for *P(q)* for common shapes such as spheres, cylinders, and ellipsoids have been developed. Here we will try fitting with these different models to see which best the describes the data. We can also double check the accuracy of assumptions and fit results by comparing the R_g calculated from the different *P(q)* fit results against the value determined from the Guinier analysis of the data.

1.2.3. Structure Factor: *S(q)*

The structure factor *S(q)* is due to interference from different objects in the sample. In a crystalline lattice, the structure factor describes the positions of different atoms in the lattice. In solution, *S(q)* is a measure of the correlation function between the center of masses of the different particles. Because the relative positions are determined by their interaction potential, *S(q)* therefore contains information on the *interactions* between objects in solution.

At low concentrations, there are no correlations between the particle positions and $S(q) \approx 1$. The scattering pattern from dilute solutions is therefore determined only by the form factor as $I(q) = AP(q)$. At higher concentrations, the interactions between the objects in solution need to be taken into consideration.

Because *S(q)* arises from interference *between different* objects, we see the effects at larger length scales which corresponds to the scattering at low q. In the limit of $q \to 0$, the scattered intensity is related to the osmotic compressibility of the system:

$$S(q \to 0) = k_B T \left(\frac{\partial n}{\partial \Pi} \right) \qquad [5]$$

Where n is the particle number density and is the Π osmotic pressure.(20) Therefore $S(q \to 0) > 1$ for attractive interactions when the system is more compressible and $S(q \to 0) < 1$ for repulsive interactions. Expressions for *S(q)* have been determined from statistical mechanical theories for the inter-particle potential. Details on how to calculate *S(q)* are beyond the scope of this write-up, but the calculated structure factors for sticky hard sphere attractive interaction as well as the repulsive hard sphere and Coulombic interactions are shown in **Fig. 7**. As can be seen in the graph, *S(q)* increases at low q for the attractive interactions and is less than 1 for repulsive interactions.
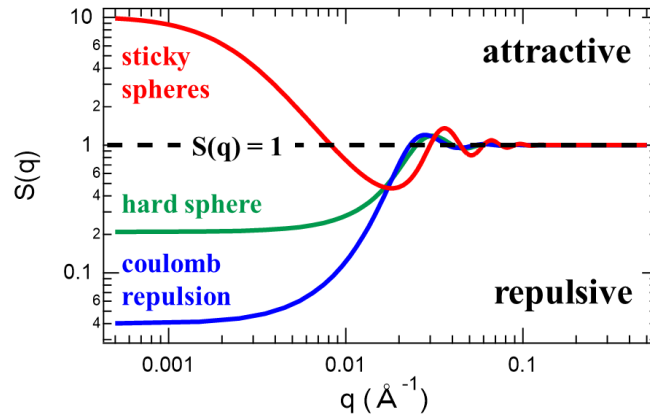
Figure 7. Calculated structure factors for sticky hard spheres (red), hard spheres (green), and charged spheres with Coulombic repulsion (blue). The calculations are for 100 nm spheres with 10% polydispersity.

Measuring the structure factor is a very powerful method for characterizing the interactions between nanoscale objects in solution. Even if we're not interested in these interactions per se, it is important to remember that the structure contributes to the measured intensity. If we are only interested in measuring the shape of our assemblies ($P(q)$), then we'll want to double check that we are in the dilute limit and $S(q) \approx 1$ for our samples. But how can we do this? The simplest way is to measure the same sample at multiple concentrations and make sure the scaled data overlap. We will perform these checks here to make sure our measured intensity is not changing with concentration, but keep in mind – this experiment assumes that the structure does not change with concentration – which may or may not be true for all amphiphiles!

2. Planning a SANS experiment

Now that we know what we are interested in measuring, how to we go about planning a successful experiment? To get good data we want to maximize the scattered intensity from our sample and minimize the background. We already introduced important things to consider for SANS sample preparation above such as making sure there is enough scattering contrast to get a good signal (Section 1.2.1) and if our samples are in a dilute limit where $S(q) \rightarrow 1$ (Section 1.2.3), but there are a few more things to think about both in terms of sample preparation and measurements before starting a SANS experiment that we discuss below.

2.1. Sample thickness

What sample thickness do we need for a SANS experiment? Choosing a sample path length not only determines the amount of sample needed for the experiment, but more importantly, the measured scattering intensity from the sample.

The intensity that we measure is proportional to the sample thickness, d_s, and sample transmission, T. Increasing d_s increases the measured intensity – but at the same time, decreases the sample

transmission. This tradeoff means that there should be an optimum d_s to maximize the measured intensity.

To find the optimum d_s, we first need to consider how increasing the thickness affects the sample transmission. The sample transmission is the fraction of neutrons that pass through the sample without being scattered or absorbed and is given by:

$$T = e^{-\Sigma_t d_s} \tag{6}$$

Where Σ_t is the total cross section and equal to the sum of the coherent, incoherent, and absorption macroscopic cross sections: $\Sigma_t = \Sigma_c + \Sigma_i + \Sigma_a$.

The absorption cross section (Σ_a) depends on the cross section of elements in the sample and can be calculated from tabulated values for the different elements if the mass density and chemical composition of the sample are known. Σ_a is wavelength dependent and increases linearly with λ for almost all wavelengths, meaning the sample transmission will also vary wavelength and must be measured for very wavelength used during the experiment (see Section 3). The incoherent cross section (Σ_i) can also be estimated from tabulated values for the different elements in the sample as well but will also depend on the atomic motions in the sample and therefore can vary slightly with temperature. Last but not least is the coherent cross section (Σ_c) which will depend on both the structure and dynamics of the material (which should not be a surprise since Σ_c is what we are aiming to measure!).

After estimating the sample transmission, the optimum sample length can be calculated because the measured intensity is proportional to

$$I_{meas} \propto d_s e^{-\Sigma_t d_s} \tag{6}$$

Which will have a maximum at $d_s = 1/\Sigma_t$. The optimum transmission, $T_{opt} = 1/e \approx 0.37$. The sample thickness that gives T_{opt} for a given sample is known as the "1/e-length".

Estimating T for our samples is straightforward but can be time consuming. Fortunately, there are tools to help. The NCNR's Web-based Neutron activation and scattering calculator (https://www.ncnr.nist.gov/resources/activation/) not only computes the scattering length density, but also estimates the incoherent and absorption cross sections and the 1/e-length for the entered materials. It is good to estimate the optimum thickness before starting a SANS experiments. In some cases, we can increase the sample thickness to get better counting statistics in shorter times or in other cases, we may need to decrease the sample thickness to prevent multiple scattering discussed next Section 2.2. Finally, it should be noted that sometimes the amount of sample available precludes optimizing the scattering volume.

2.2. Multiple scattering

It is possible to have *too* much scattering. Analyzing SANS data assumes that the neutron is only scattered *once* as it passes through the sample and that any measured scattering angle is therefore related to the structure of the sample. However, this assumption may not be true is samples that

scatter very strongly, i.e. the neutron may scatter multiple times while passing through the sample. Multiple scattering distorts the shape of the measured SANS curves and makes data analysis almost impossible. (21)

If the sample scatters too strongly, we need to consider ways to reduce the scattered intensity such as decreasing the scattering contrast $\Delta\rho^2$ or reducing the sample thickness. A good check before an experiment is to estimate Σ_i and Σ_a, because if $\Sigma_c \gg \Sigma_i + \Sigma_a$ the sample thickness should be reduced so that the transmission due to the coherent scattering remains higher than 0.9 rather than $T_{opt} = 0.37$ to avoid multiple scattering effects.

We will be using 1 mm pathlength sample cells for our experiments.

2.3. Choosing an instrument

Here at the NCNR we have a total of 5 SANS instruments: 3 SANS instruments, a very small angle scattering (VSANS) instrument, and the ultra-small angle neutron scattering (USANS) instrument. Each instrument is designed to cover a specific q-range as illustrated below in **Fig. 8**. It is important that we know the length scales of interest the sample before picking an instrument. SANS is best suited for studying samples from $\approx$ 1 nm to $\approx$ 100 nm while USANS captures length scales from $\approx$ 100 nm to $\approx$ 20 μm. VSANS bridges these two extremes and allow us to measure samples with size scales ranging from $\approx$ 1 nm to $\approx$ 1 μm.
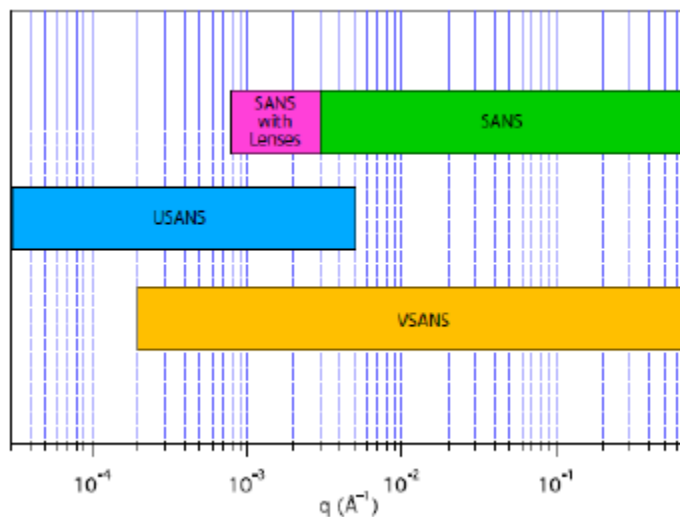

Figure 8. Comparison of the accessible q ranges for the BT-5 USANS instrument, NG-3 and NG-7 SANS instruments, and VSANS at the NCNR. The plot is reproduced from reference (22).

The cartoons in Fig. 5 suggest that a bicelle is only two molecules thick, or approximately 5 nm, so we will need to collected data at high q. However, we do not know the overall size of the bicelle, so it would be best to measure the intensity over a wide q-range to make sure we can characterize the overall size of the structures. To get a better idea of the required q-range, we can estimate the scattered intensity for the simplest case of non-interacting randomly oriented spherical particles using the spherical form factor in SasView (https://www.sasview.org/), a community-developed software package for the analysis of small angle scattering data.

Fig. 9 compares the estimated scattered intensity from spheres with radii of 5 nm and 50 nm. These calculations highlight the scattering from the smaller spheres are at higher q, and the scattering from the larger spheres is at lower q. Given the two length scales of interest in bicelles that we are studying here, *i.e.*, the bicelle thickness and radius, the scattering form these features will likely appear in different regions of q. Also note that the incoherent background (I_{inc}) present at high q will have a greater effect on the smaller features, which is another reason why we decided to prepare our samples in D_2O.
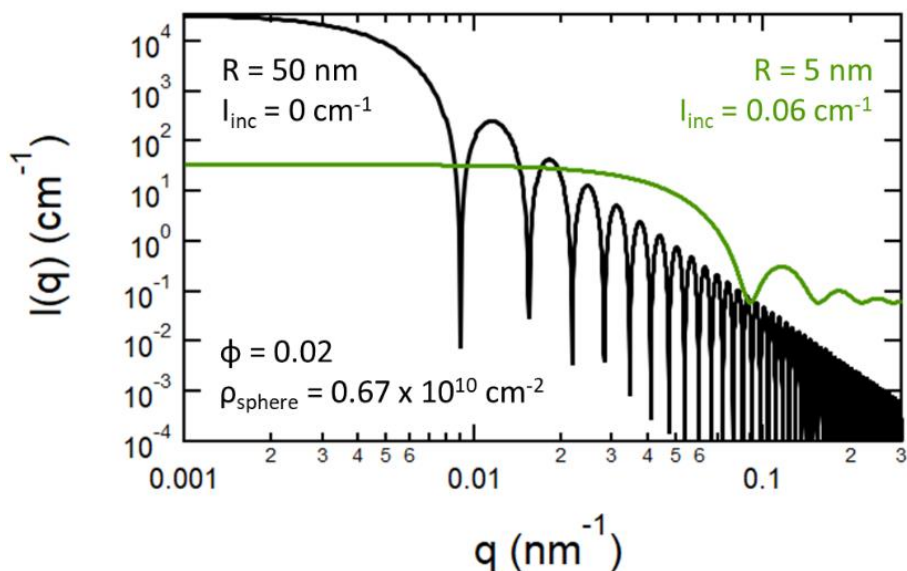

Figure 9 Estimated scattering from non-interacting spheres with an SLD of 0.67×10^{10} cm^{-2} in D_2O with different levels of incoherent background (I_{inc}). Note that I_{inc} primarily affects the data at high q. Also note that the larger spheres have a greater I_0 and scatter more strongly at low q.

Therefore, for this experiment we know we will need to measure the intensity over a wide q-range since the information we are looking for is likely distributed in the low and high q-regime. Information on the q-range of each instrument is available on the NCNR's website. If you are not sure which instrument is best for your experiment, you can always contact your friendly instrument scientists to ask! As long as you have some idea of the approximate structures and their sizes in your systems, we can help design the best possible SANS experiment.

3. Running the Experiment

After all the planning, there are a few more things to take into consideration when we start our SANS experiment. We will need to run 'backgrounds' to subtract from our sample data. We also need to figure out how long to run the measurement to ensure that the data are not too noisy and that we have good statistic when it comes time to analyze the data. Each of these topics is discussed below.

3.1. 'Backgrounds' to run

We are ultimately interested in the scattering from our sample, but there are additional measurements we need to make during a SANS experiment to correct for the "background." The neutrons counted by the detector come from 3 places: [a] neutrons scattered by the sample itself (and what we want to measure), [b] neutrons scattered by everything that is surrounding the sample as the beam passed through the sample, and [c] everything else such as stray neutrons that reach the detector without going through the sample and the electronic noise of the detector. To separate these contributions, we need to make 3 measurements during our SANS experiments:

1) Scattering from our *samples*, which will contain contributions from everything listed above (a, b and c), referred to as I_{sam} in the next section
2) Scattering from the *empty cell*, which includes scattering from everything around the sample but is not from the sample itself as well as the stray neutrons and detector sensitivity (b and c), referred to as I_{emp} in the next section
3) Counts measured with a neutron absorber in the sample position, which we call the blocked beam and will account for the stray neutrons that are measured as well as the electronic dark count (c), referred to as I_{bgd}

We also need to measure the transmission of our samples as well as the empty sample cell to correctly subtract the background measurements listed above. Remember from Section 2.1 that transmission is wavelength dependent, so we may need to measure multiple transmissions depending on how we select our instrument configurations!

3.2. How long do we need to count?

Now that we know all the measurements we need to make to be able to correctly subtract the "background" from our data – how long will we need to measure?

A SANS experiment is an example of a counting experiment where the uncertainty in the measured intensity (the standard deviation, σ, to be exact) scales with the (square root of the) total number of counts I(t): $\sigma = \sqrt{I(t)}$. The longer we measure, the more total counts we accumulate and the lower the uncertainty. A very basic rule of thumb would be to try to accumulate ≈ 200,000 from your sample *above the sample background* where the sample background may be the solvent or simply the empty cell. If the 200,000 are circularly averaged into 50 data points when plotting *I(q)* vs. *q*, then we will have about 4000 counts per data point. This averaging would mean that the standard deviation on a given point would be $\sqrt{4000} \approx 60,$ or about 1.5%, which is more than enough in most cases. In practice, most low q measurements will accumulate much fewer counts and the highest q measurements will often collect more. *It is important to remember that σ scale with $\sqrt{t}$, which means that if we needed to decrease our uncertainty by 2x from 1.5% to 0.75%, then we would need to increase out counting time by a factor of 4. Likewise cutting our time in half (in order to run more samples for example) will only increase the uncertainty by $\sqrt{2}$ or ~ 1.4x from 1.5% to ~ 2%*

Along the same lines, how long should the background and empty cell be counted relative to the sample measurement? The $\sigma = \sqrt{I(t)}$ relationships means the optimum counting times are approximately

$$\frac{t_{background}}{t_{sample}} = \sqrt{\frac{background\ count\ rate}{sample\ count\ rate}} \qquad [7]$$

If the sample scattering is weak, then the background should be counted for as long as the sample (but not longer!). But if the sample scattering is strong, say 4x that of the background, then we would need to measure the background for half the time of the sample.

4. After the experiment

After we have completed our measurements, we will need to process the raw data into a form that can be analyzed. In the next two sections we quickly review SANS data reduction and analysis.

4.1. Data reduction

What we mean by data reduction is to correct the measured scattering from the sample from the sources of background discussed in Section 3 as well as taking into consideration things such as the counting time and sample thickness to put the measured data on an absolute scale. The final data will, hopefully, have removed all the instrumental artifacts and just be the scattering cross section per unit volume which contains only the sample information of interest that we can analyze to answer the questions we set at the beginning of the experiment.

The background corrected intensity, I_{cor}, is calculated according to

$$I_{cor} = \left(I_{sam} - I_{bgd}\right) - \left(\frac{T_{sam+cell}}{T_{cell}}\right)\left(I_{emp} - I_{bgd}\right) \qquad [8]$$

And the corrected intensity is related to the differential cross section of our sample, $d\Sigma(Q)/d\Omega$ by

$$\left(\frac{d\Sigma(Q)}{d\Omega}\right)_{sam} = \frac{I_{cor}}{K\ d_s\ T_{sam+cell}} \qquad [9]$$

Where I_x denotes a measured scattering intensity, T_x a measured transmission, and d_s the sample thickness. We already talked about the different measured intensities and transmissions in

Section 3. *K* is an instrumental scale factor that is specific to the instrument set up we use to measure our desired *q* range:

$$K = \varphi \, A \, \Delta\Omega \, \varepsilon \, t \qquad\qquad [10]$$

Where:

φ = neutron flux at the sample (neutrons/cm^2/s)
A = area of incident beam on the sample
$\Delta\Omega$ = solid angle subtended by one pixel of the detector
ε = detector efficiency
t = counting time

Also note that the equation above is per pixel. The data reduction is performed on the 2D detector images, and the data are radially integrated to get *I(q)* vs. *q after* the reduction. To do this there is one other correction, shown in Fig 8, which corrects for the variation of each pixel's efficiency from the mean efficiency, ε, described above. The so-called sensitivity file is collected by the NCNR staff and not something you would worry about other than to make sure you have been given the file before you start reducing your data.

At the NCNR we use macros written by Steve Kline in IGOR Pro to perform the data reduction.(23) Details on the reduction are reduction are provided in reference (23) and written documentation and video tutorials on the reduction software are also available on the NCNR's website: https://www.ncnr.nist.gov/programs/sans/data/red_anal.html

Snapshots of the representative scattering data at the different reduction steps are also shown in **Fig. 10** on the next page
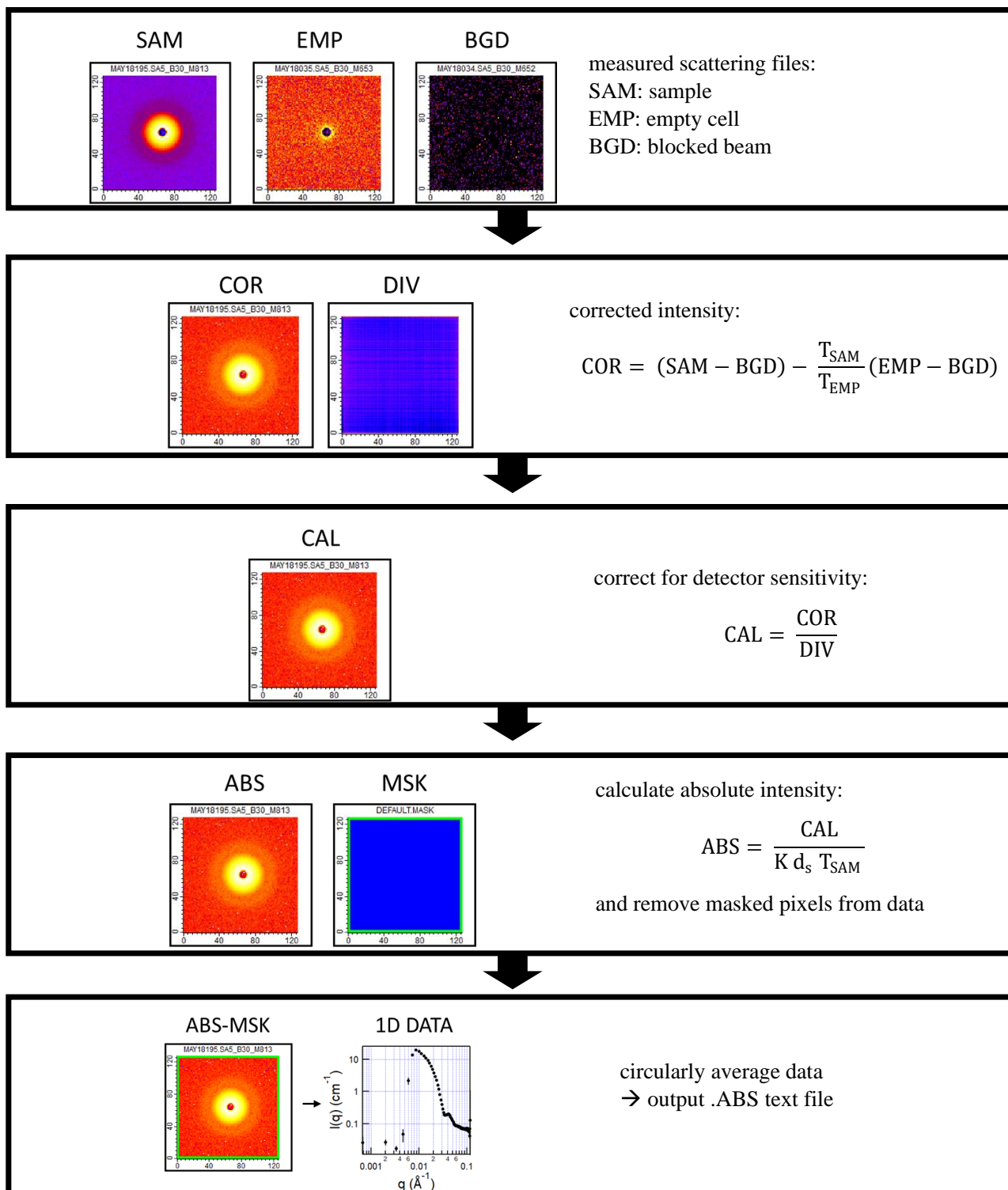
measured scattering files:
SAM: sample
EMP: empty cell
BGD: blocked beam

corrected intensity:

$$COR = (SAM - BGD) - \frac{T_{SAM}}{T_{EMP}}(EMP - BGD)$$

correct for detector sensitivity:

$$CAL = \frac{COR}{DIV}$$

calculate absolute intensity:

$$ABS = \frac{CAL}{K\, d_s\, T_{SAM}}$$

and remove masked pixels from data

circularly average data
→ output .ABS text file

Figure 10. Overview of the data reduction process with corresponding SANS data

4.2. Data analysis

At this point, we have reduced data on an absolute intensity that we can fit with models with different form factors to determine the shape of the assemblies formed by mixtures of DMPC and DHPC and where the different lipids are in these structures. Since these data no longer contain any instrumental artifacts, they can be analyzed with any available small angle scattering data analysis software package, of which there are many (see for example http://smallangle.org/content/Software). Here at the summer school we will be using SasView to model the data. SasView is an analysis software package that is developed and managed by an international collaboration of scattering facilities. More information on SasView can be found here: https://www.sasview.org/.

5. Summary and Objectives

We have covered the basics of planning a SANS experiment, performing the measurements, reducing the data, and analyzing the data. During the summer school we will analyze data from two series of experiments to answer our questions about mixtures of DMPC and DHPC:

1) Determine the form factor of the structures formed by different mixtures of DMPC and DHPC in the *dilute* limit where $S(q) \to 1$
2) Fit the data from a contrast variation experiment using d-DMPC and DHPC to determine where the different lipids are in the structures.

6. Links for helpful tools and resources

The SANS Toolbox, by Boualem Hammouda:
https://www.ncnr.nist.gov/staff/hammouda/the_SANS_toolbox.pdf

Table of scattering lengths:
https://www.ncnr.nist.gov/resources/n-lengths/

SLD Calculator:
https://www.ncnr.nist.gov/resources/activation/

Video documentation on the NCNR's data reduction by Steve Kline:
https://www.ncnr.nist.gov/programs/sans/data/movies/reduction_analysis_movies.html

SASView:
https://www.sasview.org/

7. References

1. Prosser RS, Evanics F, Kitevski JL, & Al-Abdul-Wahid MS (2006) Current Applications of Bicelles in NMR Studies of Membrane-Associated Amphiphiles and Proteins. *Biochemistry* 45(28):8453-8465.
2. Dufourc EJ (2021) Bicelles and nanodiscs for biophysical chemistry11A tribute to Prof Michèle Auger, University Laval, Canada. *Biochimica et Biophysica Acta (BBA) - Biomembranes* 1863(1):183478.
3. Faham S & Bowie JU (2002) Bicelle crystallization: a new method for crystallizing membrane proteins yields a monomeric bacteriorhodopsin structure11Edited by D. Rees. *Journal of Molecular Biology* 316(1):1-6.
4. Ujwal R & Bowie JU (2011) Crystallizing membrane proteins using lipidic bicelles. *Methods* 55(4):337-341.
5. Barbosa-Barros L*, et al.* (2012) Bicelles: Lipid Nanostructured Platforms with Potential Dermal Applications. *Small* 8(6):807-818.
6. Katsaras J, Harroun TA, Pencer J, & Nieh M-P (2005) "Bicellar" Lipid Mixtures as used in Biochemical and Biophysical Studies. *Naturwissenschaften* 92(8):355-366.
7. Anonymous (*Micelles, Membranes, Microemulsions, and Monolayers* (Springer).
8. Tanford C (1973) *The Hydro-Phobic Effect: Formation of Micelles and Biological Membranes* (Wiley, New York).
9. Israelachvili JN, Mitchell DJ, & Ninham BW (1976) Theory of self-assembly of hydrocarbon amphiphiles into micelles and bilayers. *Journal of the Chemical Society, Faraday Transactions 2: Molecular and Chemical Physics* 72(0):1525-1568.
10. Israelachvili J (2006) *Intermolecular & Surface Forces* (Academic Press).
11. Kučerka N*, et al.* (2005) Structure of Fully Hydrated Fluid Phase DMPC and DLPC Lipid Bilayers Using X-Ray Scattering from Oriented Multilamellar Arrays and from Unilamellar Vesicles. *Biophysical Journal* 88(4):2626-2637.
12. Lin TL, Chen SH, Gabriel NE, & Roberts MF (1987) Small-angle neutron scattering techniques applied to the study of polydisperse rodlike diheptanoylphosphatidylcholine micelles. *The Journal of Physical Chemistry* 91(2):406-413.
13. Hoffmann H, Thunig C, Munkert U, Meyer HW, & Richter W (1992) From vesicles to the L3 (sponge) phase in alkyldimethylamine oxide/heptanol systems. *Langmuir* 8(11):2629-2638.
14. Khan A (1996) Phase science of surfactants. *Current Opinion in Colloid & Interface Science* 1(5):614-623.
15. Sanders CR & Landis GC (1995) Reconstitution of Membrane Proteins into Lipid-Rich Bilayered Mixed Micelles for NMR Studies. *Biochemistry* 34(12):4030-4040.
16. Prosser RS, Hwang JS, & Vold RR (1998) Magnetically Aligned Phospholipid Bilayers with Positive Ordering: A New Model Membrane System. *Biophysical Journal* 74(5):2405-2418.
17. Triba MN, Warschawski DE, & Devaux PF (2005) Reinvestigation by Phosphorus NMR of Lipid Distribution in Bicelles. *Biophysical Journal* 88(3):1887-1901.
18. Jiang Y & Kindt JT (2007) Simulations of edge behavior in a mixed-lipid bilayer: Fluctuation analysis. *The Journal of Chemical Physics* 126(4):045105.
19. Caldwell TA*, et al.* (2018) Low-q Bicelles Are Mixed Micelles. *The Journal of Physical Chemistry Letters* 9(15):4469-4473.
20. Chang J*, et al.* (1995) Structural and Thermodynamic Properties of Charged Silica Dispersions. *The Journal of Physical Chemistry* 99(43):15993-16001.
21. Schelten J & Schmatz W (1980) Multiple-scattering treatment for small-angle scattering problems. *Journal of Applied Crystallography* 13(4):385-390.
22. Liu Y, Yuan G, & Bleuel M (2014) *Gelation of spherical colloidal systems with bridging attractions*.
23. Kline S (2006) Reduction and analysis of SANS and USANS data using IGOR Pro. *Journal of Applied Crystallography* 39(6):895-900.